Supplement of Biogeosciences, 21, 1639–1673, 2024
https://doi.org/10.5194/bg-21-1639-2024-supplement

Biogeosciences
Open Access

Supplement of

Seasonality and response of ocean acidification and hypoxia to major environmental anomalies in the southern Salish Sea, North America (2014–2018)

Simone R. Alin et al.

Correspondence to: Simone R. Alin (simone.r.alin@noaa.gov)

S1 Methods: Details regarding seacarb calculations, including differences between calculated parameters using different dissociation and thermodynamic constants, fCO_2 vs. pCO_2, and Ω_{arag} vs. Ω_{calc}

Within seacarb, input parameters from the Salish cruise compiled data set were DIC (DIC_UMOL_KG), TA (TA_UMOL_KG), phosphate (PHOSPHATE_UMOL_KG), and silicate (SILICATE_UMOL_KG) content values from bottle samples analyzed in the laboratory, along with CTD measurements of temperature (CTDTMP_DEG_C_ITS90), salinity (CTDSAL_PSS78), and pressure (CTDPRS_DBAR). To conform with the default units of seacarb, all input content data were first divided by 10^6 to convert from µmol kg^{-1} to mol kg^{-1}, and pressure (dbar) values were divided by 10 to convert to bar.

For end users using dissociation constants explicitly targeted to the broader salinity ranges seen in the Salish Sea for their own measurements, we did two sets of calculations, using Lueker et al. (2000, "L00") and Waters et al. (2014, "W14") dissociation constants, with all other seacarb options the same as described in the main text. Comparison of the results showed that the average differences in calculated values using L00 rather than W14 constants (i.e., L00 – W14) were –0.003±0.002 for pH_T, +5.0±1.3 µatm for fCO_2 (+5.1±1.4 for pCO_2), and –0.001 for Ω_{arag} and Ω_{calc} (±0.003 and ±0.004, respectively). Only two samples of the 4021 with good analytical values for all analytical input parameters had salinity <19—the lower end of the salinity range appropriate for use with L00 constants, and thus generated warning flags. Thus, our use of the L00 constants would not have a discernible effect on the results discussed here.

For the L00 vs. W14 comparison, we used the TEOS-10 thermodynamic seawater equations with both sets of carbonate system dissociation constants. However, prior WCOA cruise publications used EOS-80 seawater equations, whereas we used the more recent TEOS-10 equations, in keeping with current recommendations (IOC, SCOR, and IAPSO, 2010; Jiang et al., 2022). The differences between paired calculated carbonate system parameters caused by using EOS-80 vs. TEOS-10 thermodynamic seawater equations with the L00 dissociation constants were similar in magnitude, with average offsets (i.e., EOS-80 – TEOS-10) of –0.003 for pH_T, +5.2 µatm for fCO_2, 0.000 for Ω_{arag}, and –0.001 for Ω_{calc}.

To facilitate comparisons between fCO_2 values and pCO_2 values from other data sources or publications, the average difference between the two values (i.e., $pCO_2 - fCO_2$ because pCO_2 is always larger because it does not take into account interactions between CO_2 and other molecules) in this data compilation is 22.5 µatm across all pairs of seawater and carbonate system thermodynamic constants. The difference increased with fCO_2 level, with fCO_2 values averaging 2.8 µatm lower than pCO_2 at 0–499 µatm, 17.7 µatm at 500–999 µatm, 43.4 µatm at 1000–1999 µatm, and 55.7 µatm at >2000 µatm.

Finally, a regression between Ω_{arag} and Ω_{calc} indicated that Ω_{calc} was 1.59 times Ω_{arag} in the Salish cruise data package, which is a slightly larger coefficient than reported for the relationship between the two parameters by Mucci (1983), presumably to different temperature and salinity characteristics of our regional water masses.

Supplemental figures, with captions

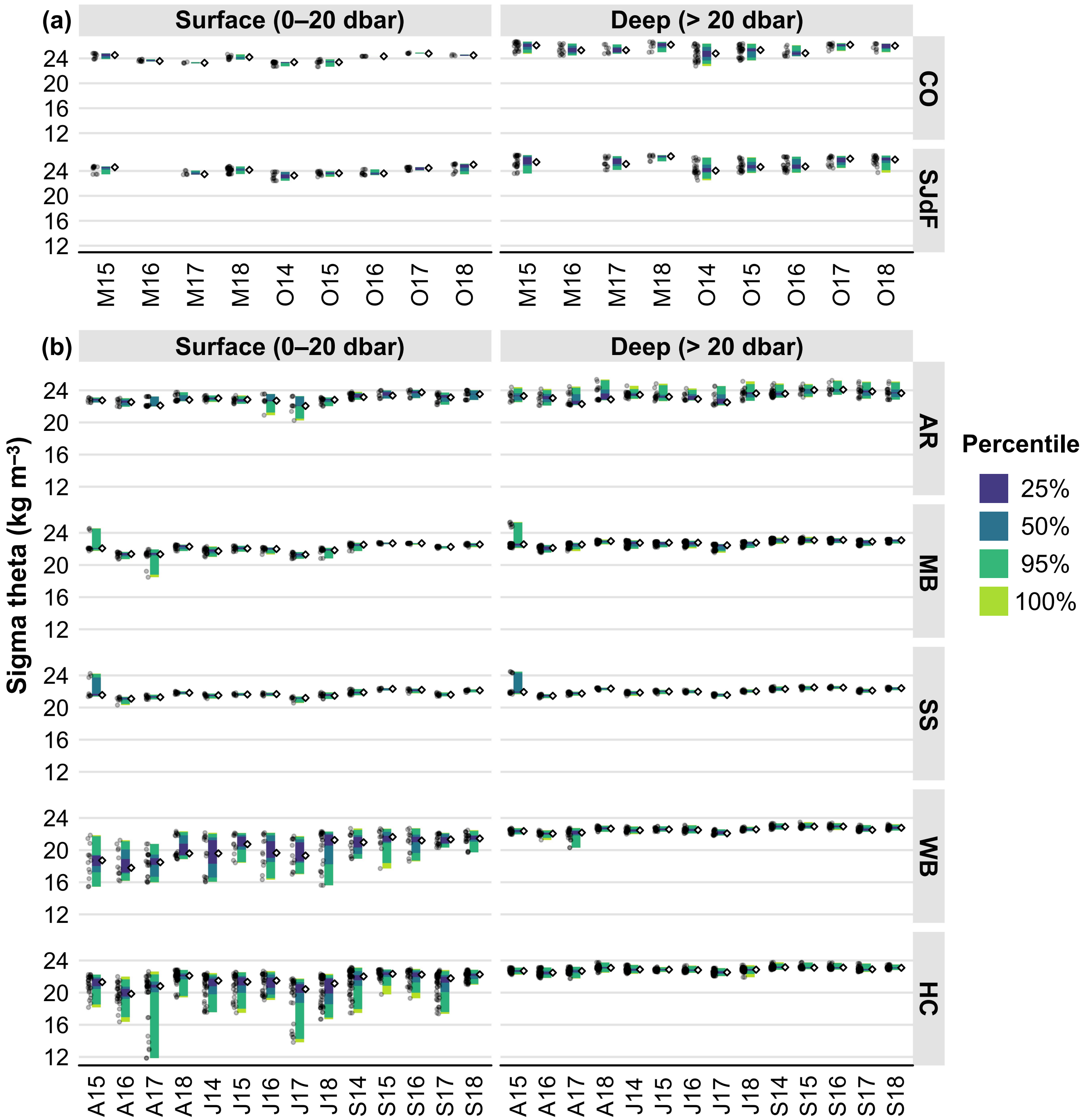

Figure S1: Raincloud plots for potential density anomalies (σ_θ) in a) coastal (CO) and Strait of Juan de Fuca (SJdF) Sound-to-Sea surveys in the early and late upwelling season (May and October, respectively) and b) Puget Sound (PS) surveys during April, July, and September beginning in the summer of 2014. PS basins are Admiralty Reach (AR), Main Basin (MB), South Sound (SS), Whidbey Basin (WB), and Hood Canal (HC). Figure organization is the same as in Figures 3–4, 6, and 8–9 in the main text.

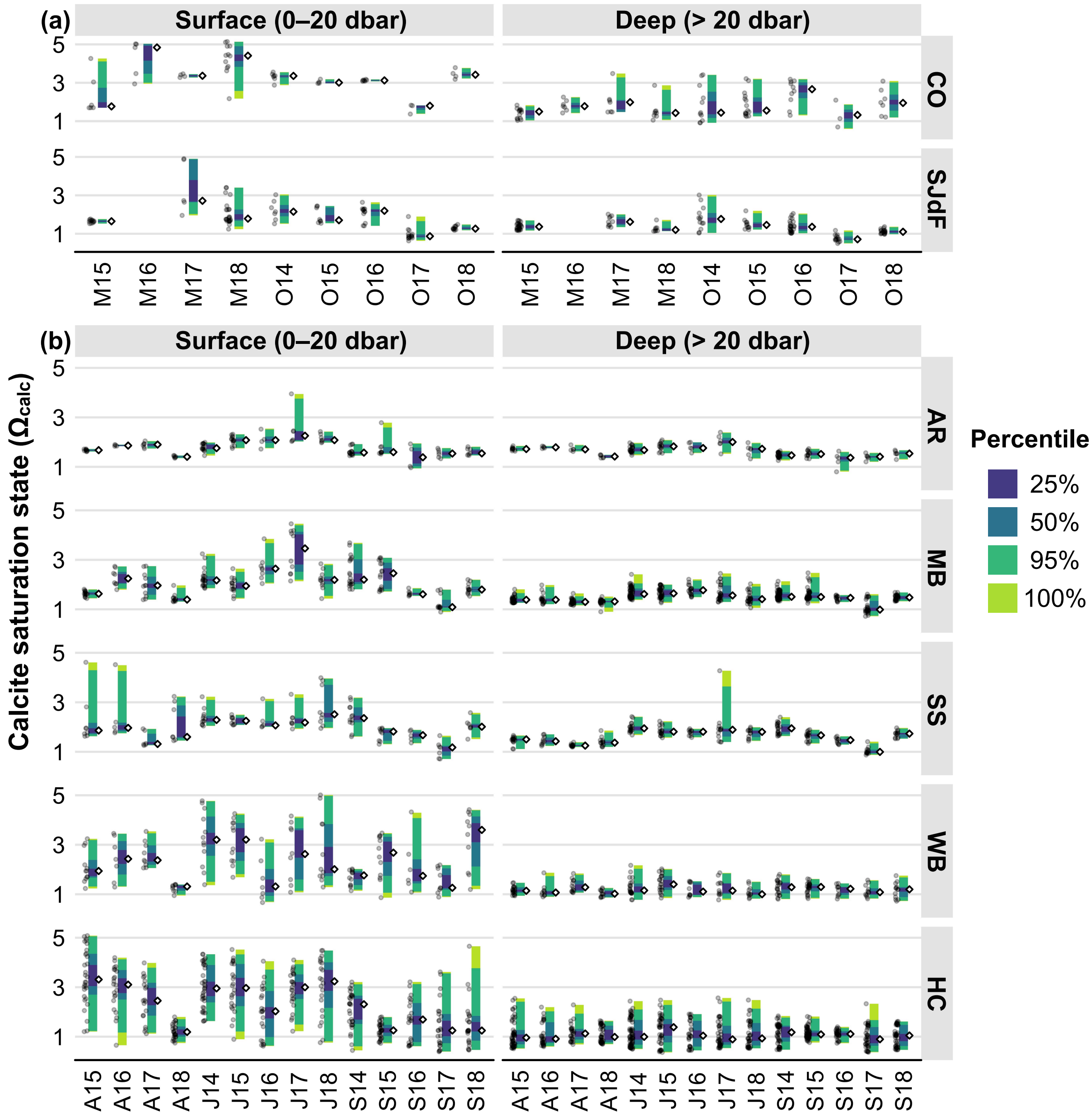

Figure S2: Raincloud plots for calcite saturation state (Ω_{calc}). Figure organization is as described in Figure S1.

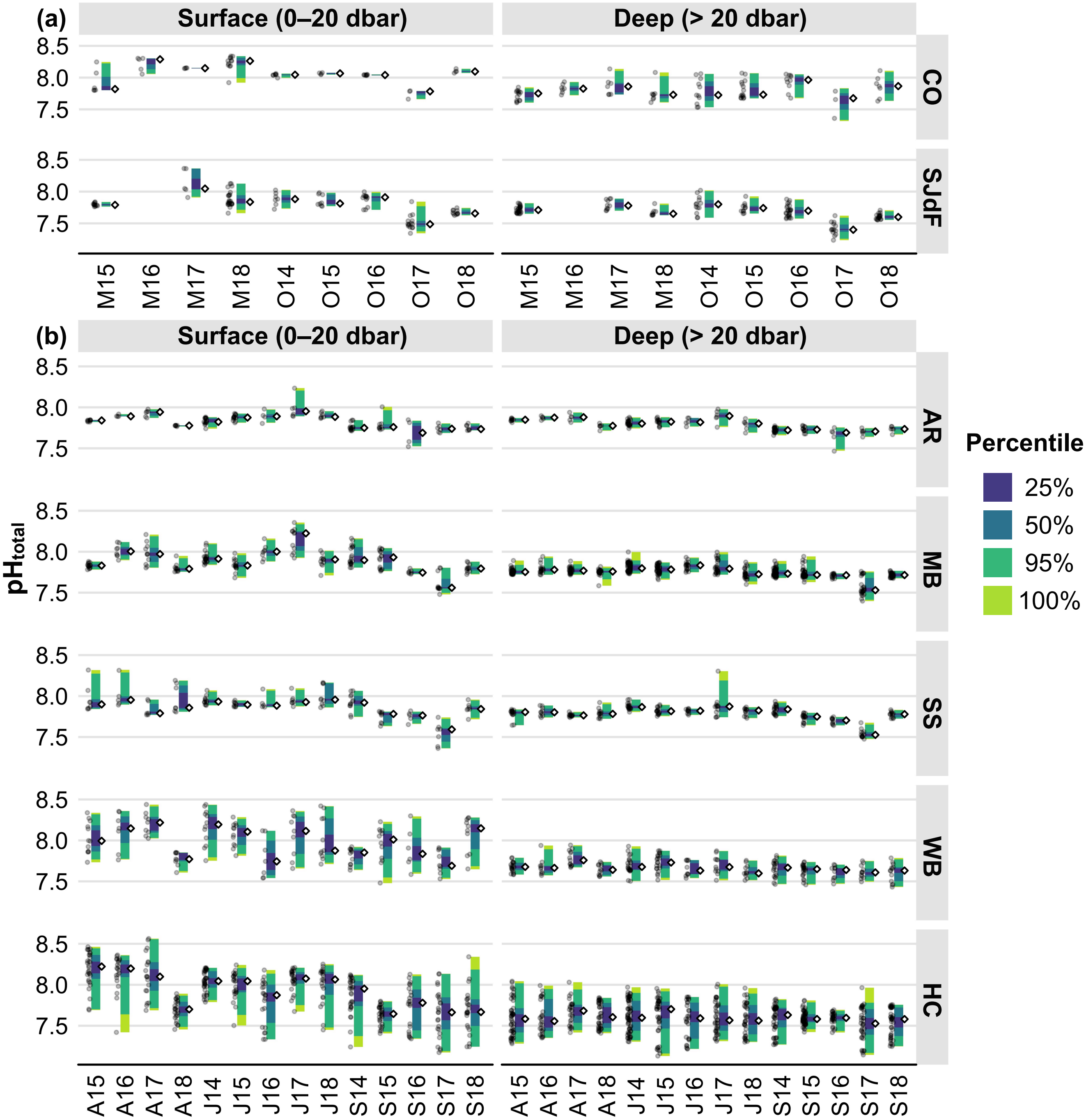

Figure S3: Raincloud plots for pH on the total scale (pH_{total}). Figure organization is as described in Figure S1.

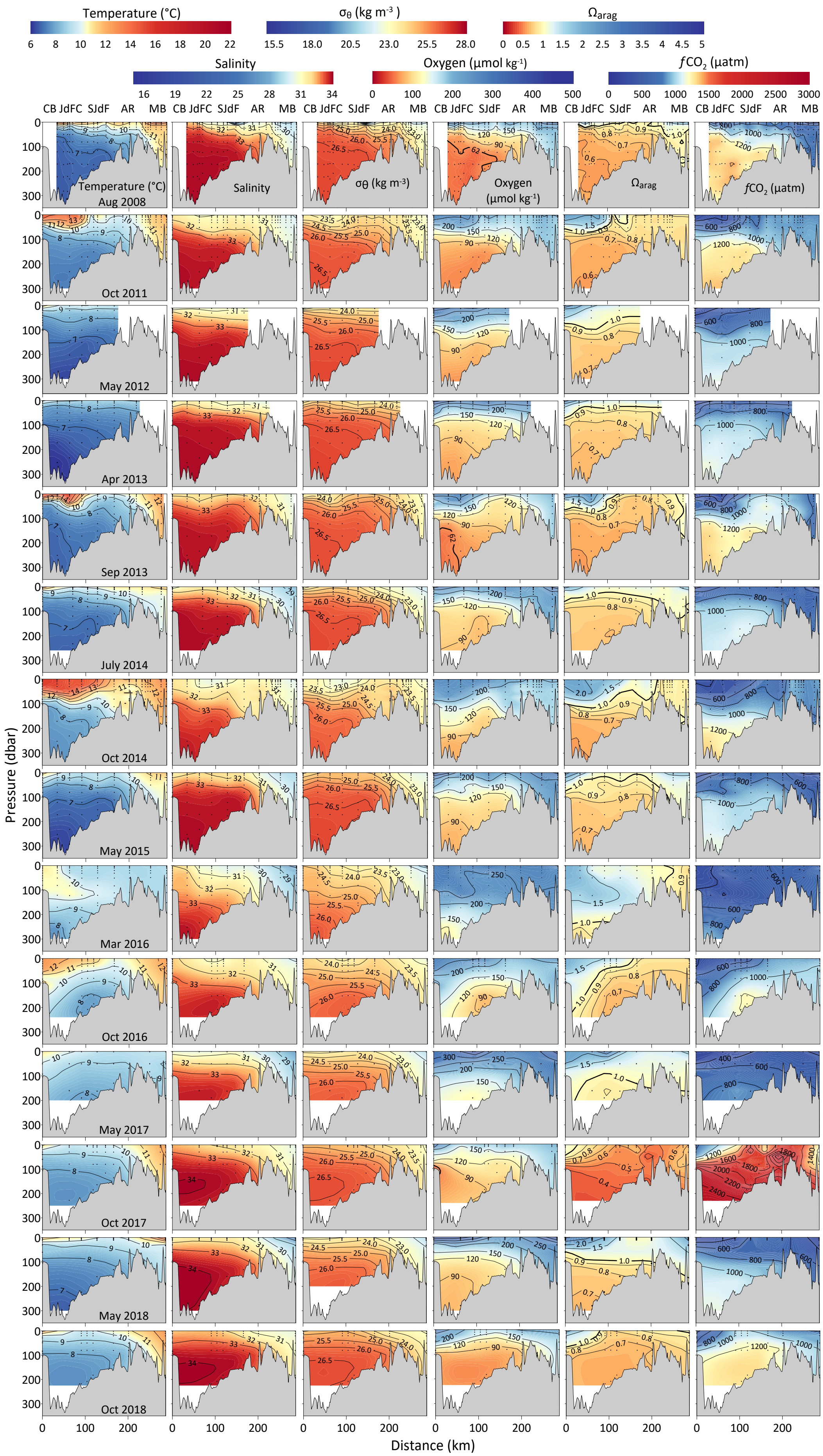

Temperature (°C)
6 8 10 12 14 16 18 20 22
σθ (kg m-3)
15.5 18.0 20.5 23.0 25.5 28.0
Ωarag
0 0.5 1 1.5 2 2.5 3 3.5 4 4.5 5
Salinity
16 19 22 25 28 31 34
Oxygen (µmol kg-1)
0 100 200 300 400 500
ƒCO2 (µatm)
0 500 1000 1500 2000 2500 3000
CB JdFC SJdF AR MB
Temperature (°C)
Salinity
σθ (kg m-3)
Oxygen (µmol kg-1)
Ωarag
ƒCO2 (µatm)
Aug 2008
Oct 2011
May 2012
Apr 2013
Sep 2013
July 2014
Oct 2014
May 2015
Mar 2016
Oct 2016
May 2017
Oct 2017
May 2018
Oct 2018
Pressure (dbar)
Distance (km)

Figure S4: Depth transect plots from Sound-to-Sea cruises for CTD temperature, salinity, potential density anomaly, adjusted CTD oxygen, aragonite saturation state (Ω_{arag}), and CO_2 fugacity (fCO_2) in respective columns. The month and year when each cruise began is indicated in left panel of each row. Each panel shows ocean conditions starting at the Ćháʔba· mooring (CB), traveling through the Juan de Fuca Canyon (JdFC) and the Strait of Juan de Fuca (SJdF), over the glacial sills in Admiralty Reach (AR), and into the Main Basin (MB) of Puget Sound as the distance along transect increases (see map in Figure 1). Color scales for fCO_2 and Ω_{arag} are the same as in the comparable Puget Sound figures (Figures S5–S6). Similarly, color scales for temperature, salinity, and oxygen are the same as for Figs. 4–6 and 9 in the Alin et al. (2024) companion article.

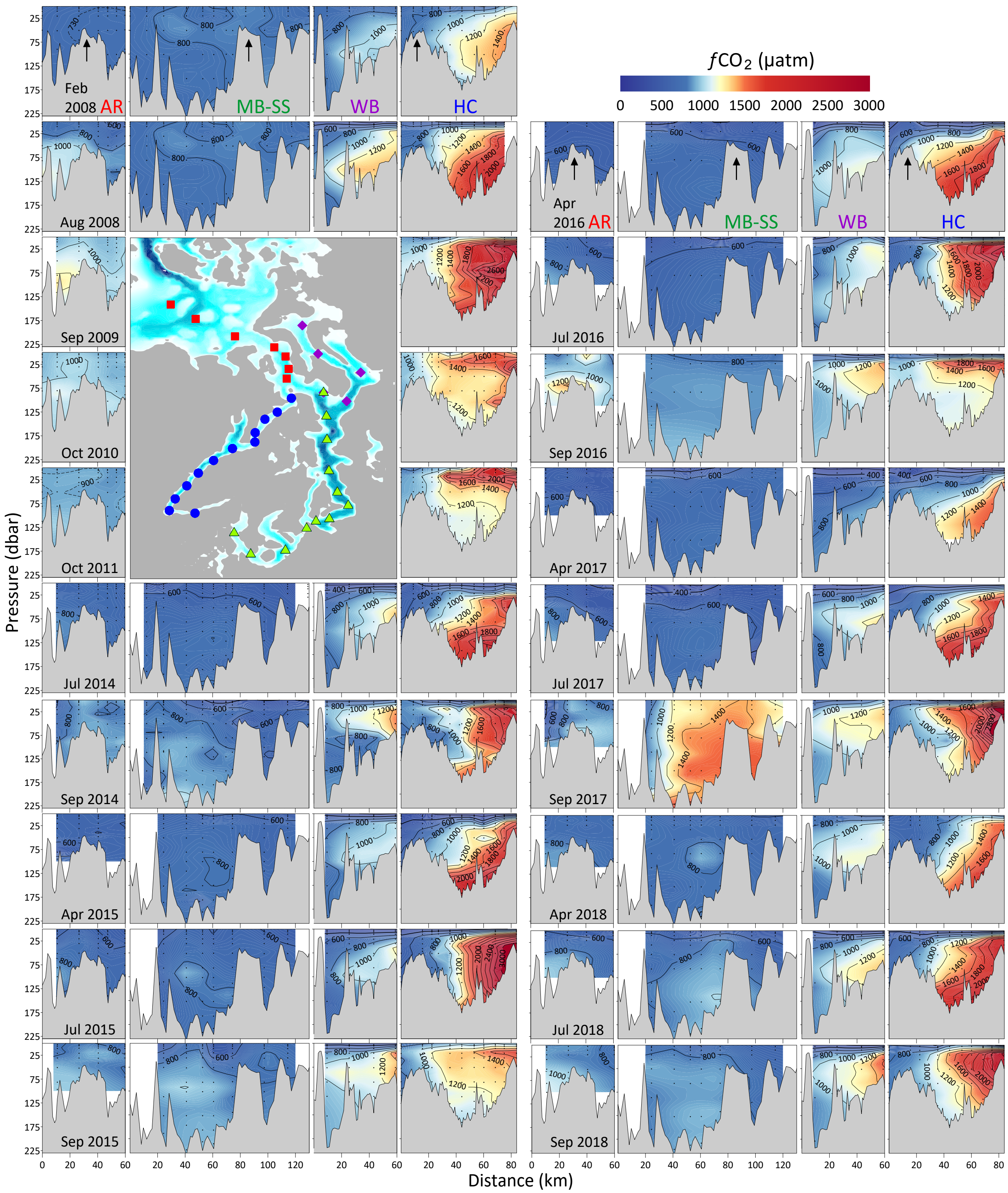

Figure S5: Depth transect plots from all Puget Sound cruises by sub-basin for calculated CO_2 fugacity values (fCO_2, µatm), with the month and year when each cruise began indicated in the left panel of each row, noting that there are two columns consisting of four panels each to encompass all cruises. From left to right, panels within each column correspond to Admiralty Reach (AR), Main Basin–South Sound (MB–SS), Whidbey Basin (WB), and Hood Canal (HC). Colours of abbreviations correspond to station colours in Figure 1. Admiralty Reach panels show the bathymetric profile and ocean conditions from the Strait of Juan de Fuca (SJdF) on the left going through Admiralty Reach toward Puget Sound on the right. The other three panels start at the nearest point on their respective transects inside Puget Sound from Admiralty Reach and progress to the distal end of the transects shown in the Figure 1 inset map as distance along transect increases.

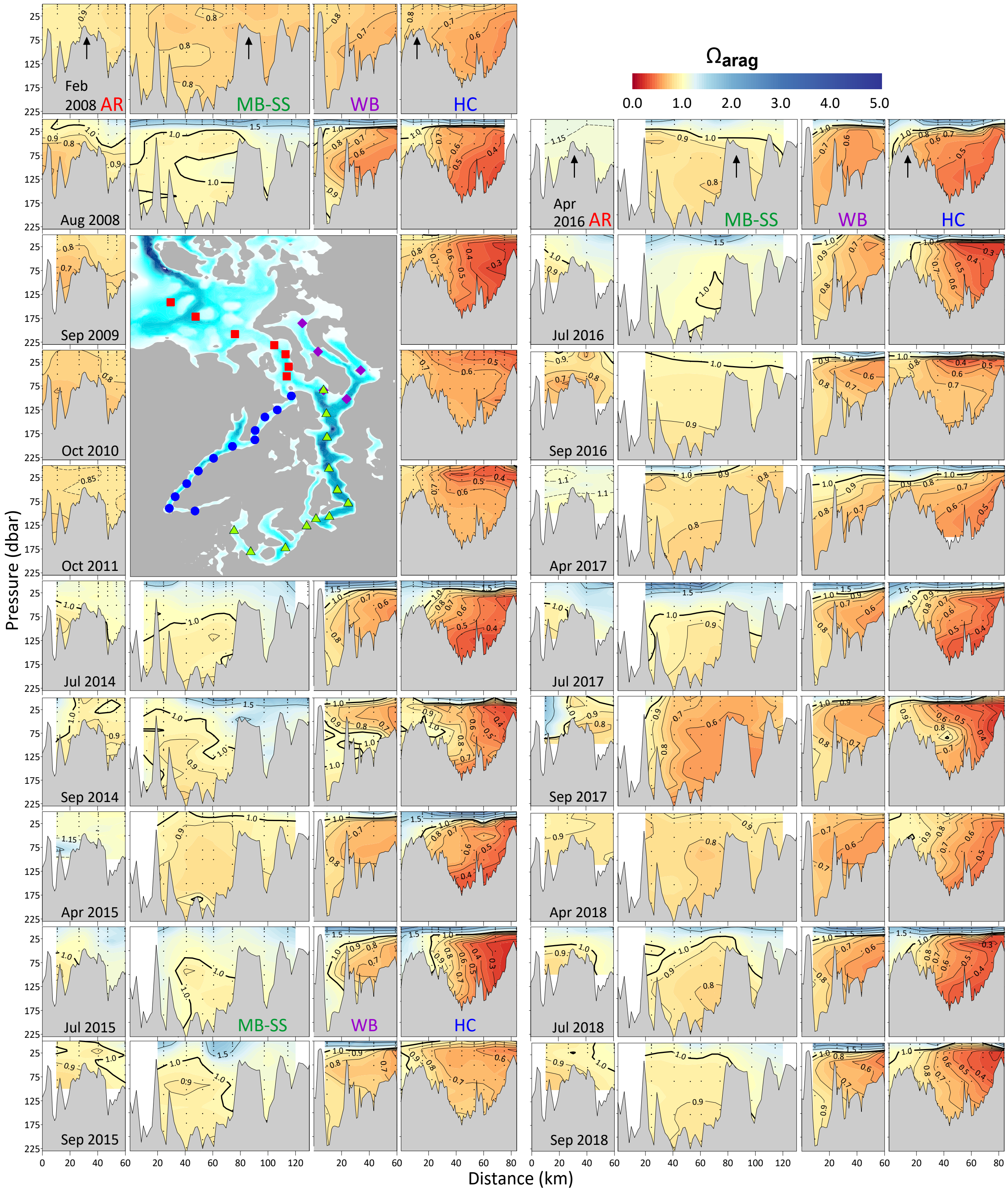

Figure S6: Depth transect plots from all Puget Sound cruises for aragonite saturation state (Ω_{arag}). Figure organization is the same as in Figure S5.

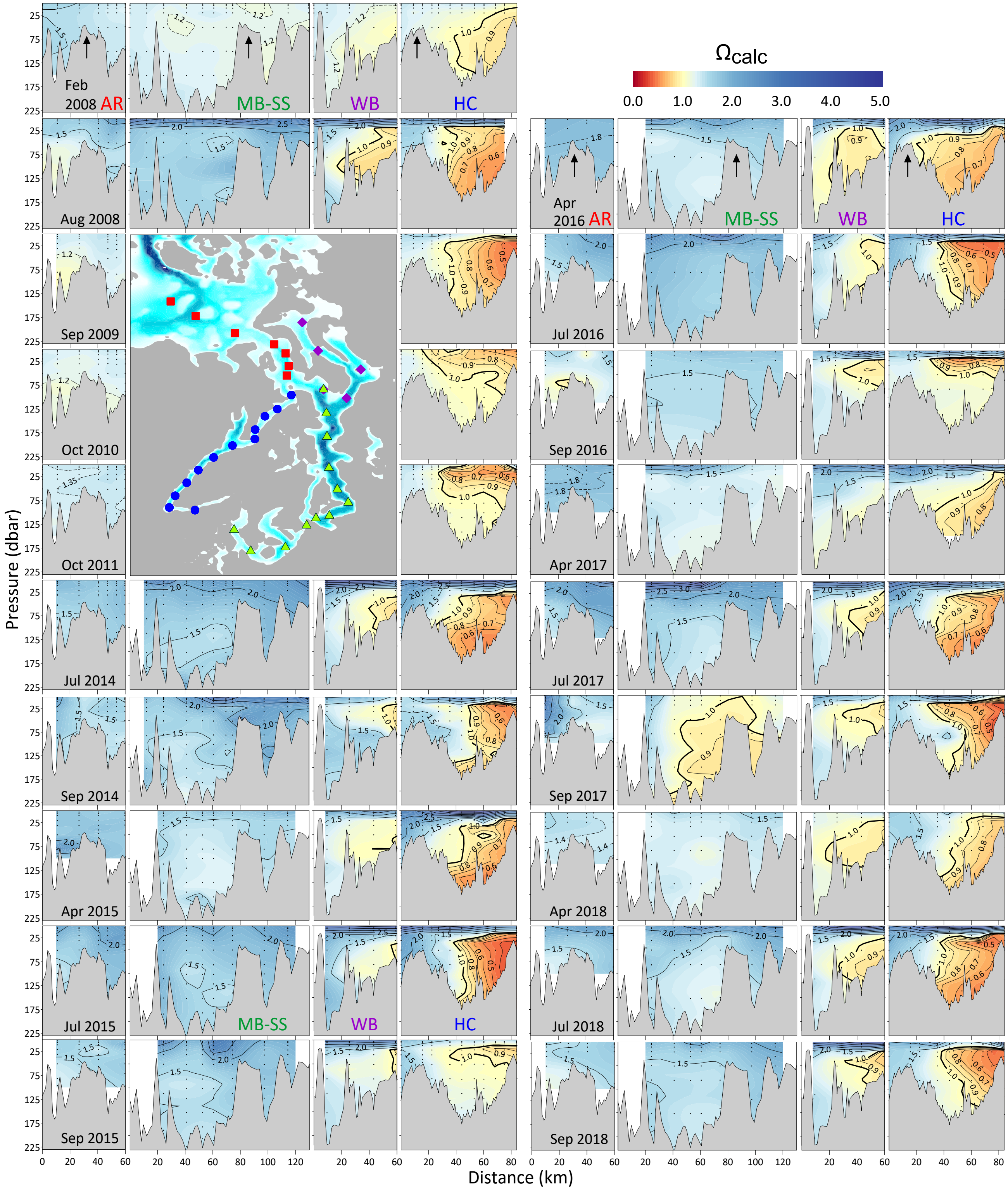

Figure S7: Depth transect plots from all Puget Sound cruises for calcite saturation state (Ω_{calc}). Figure organization is the same as in Figure S5.

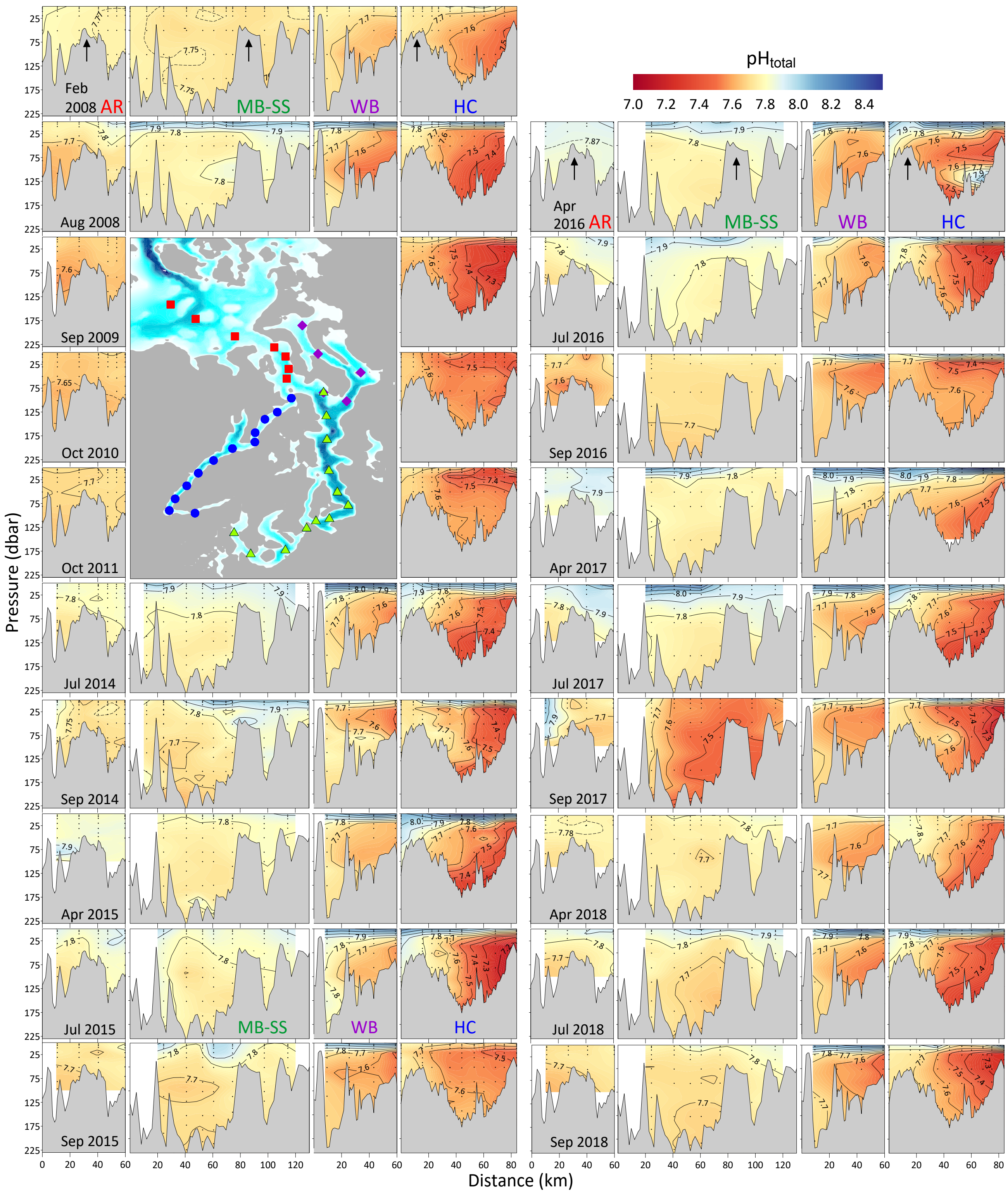

Figure S8: Depth transect plots from all Puget Sound cruises for pH on the total scale (pH_T). Figure organization is the same as in Figure S5.

References Cited

Alin, S. R., Newton, J. A., Feely, R. A., Greeley, D., Curry, B., Herndon, J., and Warner, M.: A decade-long cruise time series (2008–2018) of physical and biogeochemical conditions in the southern Salish Sea, North America, Earth Syst. Sci. Data, 16, 837–865, https://doi.org/10.5194/essd-16-837-2024, 2024

IOC, SCOR, and IAPSO: The international thermodynamic equation of seawater – 2010: Calculation and use of thermodynamic properties, Intergovernmental Oceanographic Commission, UNESCO, 2010.

Jiang, L.-Q., Pierrot, D., Wanninkhof, R., Feely, R. A., Tilbrook, B., Alin, S., Barbero, L., Byrne, R. H., Carter, B. R., Dickson, A. G., Gattuso, J.-P., and Greeley, D.: Best Practice Data Standards for Discrete Chemical Oceanographic Observations, Frontiers in Marine Science, 8, 705638, https://doi.org/10.3389/fmars.2021.705638, 2022.

Lueker, T. J., Dickson, A. G., and Keeling, C. D.: Ocean pCO_2 calculated from dissolved inorganic carbon, alkalinity, and equations for K_1 and K_2: validation based on laboratory measurements of CO_2 in gas and seawater at equilibrium, Marine Chemistry, 70, 105–119, https://doi.org/10.1016/S0304-4203(00)00022-0, 2000.

Mucci, A.: The solubility of calcite and aragonite in seawater at various salinities, temperatures, and one atmosphere total pressure, American Journal of Science, 283, 780–799, 1983.

Waters, J., Millero, F. J., and Woosley, R. J.: Corrigendum to "The free proton concentration scale for seawater pH", [MARCHE: 149 (2013) 8–22], Marine Chemistry, 165, 66–67, https://doi.org/10.1016/j.marchem.2014.07.004, 2014.